

THE ENVIRONMENTS OF LOW AND HIGH LUMINOSITY RADIO GALAXIES AT MODERATE REDSHIFTS

M. W. AUGER, R. H. BECKER, C. D. FASSNACHT

Department of Physics, University of California, 1 Shields Avenue, Davis, CA 95616, USA

(Accepted 2007 December 26)

ABSTRACT

In the local Universe, high-power radio galaxies live in lower density environments than low-luminosity radio galaxies. If this trend continues to higher redshifts, powerful radio galaxies would serve as efficient probes of moderate redshift groups and poor clusters. Photometric studies of radio galaxies at $0.3 \lesssim z \lesssim 0.5$ suggest that the radio luminosity-environment correlation disappears at moderate redshifts, though this could be the result of foreground/background contamination affecting the photometric measures of environment. We have obtained multi-object spectroscopy of in the fields of 14 lower luminosity ($L_{1.4 \text{ GHz}} < 4 \times 10^{24} \text{ W Hz}^{-1}$) and higher luminosity ($L_{1.4 \text{ GHz}} > 1.2 \times 10^{25} \text{ W Hz}^{-1}$) radio galaxies at $z \approx 0.3$ to spectroscopically investigate the link between the environment and the radio luminosity of radio galaxies at moderate redshifts. Our results support the photometric analyses; there does not appear to be a correlation between the luminosity of a radio galaxy and its environment at moderate redshifts. Hence, radio galaxies are not efficient signposts for group environments at moderate redshifts.

Subject headings:

1. INTRODUCTION

Photometric studies of radio galaxies have shown that Fanaroff-Riley type I (FR I; Fanaroff & Riley 1974) (low luminosity and edge-dimmed radio lobes) and FR II (high luminosity and edge-brightened lobes) radio galaxies exist in different environments in the local Universe; FR I galaxies reside in rich clusters while FR II galaxies tend to inhabit poor clusters or rich groups (e.g., Heckman et al. 1986; Prestage & Peacock 1988; Lilly & Prestage 1987). Studies of higher redshift radio galaxies indicate that this difference disappears at moderate redshifts ($z \sim 0.5$), where both FR types are associated with cluster-like environments (e.g., Hill & Lilly 1991; Bahcall & Chokshi 1992; Allington-Smith et al. 1993). In contrast, Zirbel (1997) suggests that, although the environments of both types of galaxies are more dense at moderate redshifts than low redshifts, the environments of FR II galaxies remain less dense than FR I sources out to $z \sim 0.5$. Only the low redshift trend of FR I environments being more dense than the environments of FR II galaxies has been confirmed with X-ray observations (Miller et al. 1999) and optical spectroscopy (Miller et al. 2002). It is quite difficult to detect and characterize group-like over-densities at moderate redshifts without spectroscopy. Photometric properties are difficult to use because groups tend not to have substantial bright early-type populations (e.g., Wilman et al. 2005) that form a red sequence, and foreground and background interlopers are common. Therefore, field spectroscopy is necessary to determine whether FR II galaxies may be useful signposts to identify moderate redshift galaxy groups.

These galaxy groups and poor clusters are excellent laboratories for studying galaxy evolution. Over half of all galaxies in the local Universe are members of groups (Huchra & Geller 1982; Tully 1987), and these groups have moderate densities

and low velocity dispersions that make them the preferred environments for dynamic galaxy evolution (e.g., Zabludoff & Mulchaey 1998; Carlberg et al. 2001b; Aarseth & Fall 1980; Barnes 1985) compared to clusters or the field (e.g., Aceves & Velázquez 2002; Lin et al. 2004; Conselice et al. 2003; Patton et al. 2002). Though cluster cores also promote some galaxy processing and evolution, the high velocity dispersions associated with these cores decrease the effective interaction cross-section between galaxies and limit the evolutionary effects of galaxy-galaxy interactions (e.g., Bower & Balogh 2004). Therefore galaxy groups provide excellent conditions for studying interactions that affect the star formation rate of galaxies and AGN ignition (e.g., Mihos et al. 1992; Iono et al. 2004; Bahcall et al. 1997; Best 2004).

The most significant obstacle to studying galaxy evolution in group environments is identifying non-local groups. The Sloan Digital Sky Survey (SDSS; York et al. 2000) and the 2 Degree Field Galaxy Redshift Survey (2dFGRS; Colless et al. 2001) have extended local group samples (e.g., Ramella et al. 1989; Zabludoff & Mulchaey 1998) to redshifts $z \sim 0.2$ (e.g., Weinmann et al. 2006; Collister & Lahav 2005; Padilla et al. 2004). Blind redshift surveys at higher redshifts have successfully identified galaxy groups to $z \sim 0.7$ (e.g., Wilman et al. 2005; Gerke et al. 2005), but the substantial amount of telescope time invested in these surveys makes it desirable to find alternative methods of identifying moderate redshift groups. Mulchaey et al. (2006) use deep X-ray observations to select groups at moderate redshifts, though this method may preferentially select the most massive groups. Gravitational lenses have also been used to identify moderate redshift groups (Momcheva et al. 2006; Williams et al. 2006; Auger et al. 2007, 2008; Fassnacht et al. 2007), though the scarcity of lenses limits the utility of this method. Radio galaxies have been used extensively to find high redshift clusters (e.g., Deltorn et al. 1997; Blanton et al. 2001, 2003) and protoclusters (e.g.,

Miley et al. 2006; Venemans et al. 2007), but the FR I/FR II environment dichotomy suggests that they may also be useful for identifying less rich galaxy groups (e.g., Allington-Smith et al. 1993).

In this paper we present spectroscopic observations of the fields of a sample of 14 moderate redshift radio galaxies. We investigate the relationship between the radio luminosity and spectroscopic group properties, and we analyze the effectiveness of using high luminosity radio galaxies to preferentially locate moderate redshift groups. Throughout this paper we assume a radio spectral index of $\alpha = 0.5$, where $S_\nu \propto \nu^{-\alpha}$, and we use a Λ CDM cosmology with $\Omega_\Lambda = 0.73$ and $\Omega_M = 0.27$.

2. RADIO GALAXY SAMPLE

We have used the SDSS and FIRST survey (Becker et al. 1995) to identify a sample of moderate redshift radio galaxies. The sources in the FIRST catalog were matched against the galaxies in the SDSS DR 5 spectroscopic catalog (Adelman-McCarthy et al. 2007) with a conservative matching tolerance of $1''$; 99.9% of these matches are real, as determined by comparing the number of matches from the two catalogs to the number of matches between the SDSS and a pseudo-random radio catalog (the FIRST catalog with a $2'$ offset applied to all sources). The resulting matched catalog was then searched for all objects that had at least two additional FIRST sources within $60''$ of the host galaxy. These sources were all reviewed by eye to morphologically identify ‘classical’ FR I and FR II sources. Note that our radio galaxy catalog differs slightly from the usual definition of FR I and FR II sources, as all of our radio galaxies also have radio cores.

The radio luminosities of these galaxies were determined by summing the fluxes of all detected FIRST components that are part of the radio galaxy. We also summed the fluxes of NVSS (Condon et al. 1998) sources, and we choose the larger of the FIRST/NVSS values to assign the radio luminosity to the galaxy; this allows us to account for the sensitivity differences of the surveys and for the possibility of flux being resolved out of the FIRST images. The radio galaxies were then divided into lower luminosity ($L_{1.4 \text{ GHz}} < 4 \times 10^{24} \text{ W Hz}^{-1}$) and higher luminosity ($L_{1.4 \text{ GHz}} > 1.2 \times 10^{25} \text{ W Hz}^{-1}$) subsamples. The high luminosity criterion is motivated by previous studies of powerful radio galaxies (e.g., Zirbel 1997), while the low luminosity criterion was chosen to provide a reasonable number of sources (given the depth of the FIRST survey at $z \approx 0.35$) and to be well-separated from the high luminosity sample. Multi-object spectroscopy was obtained for the fields of the 14 targets that were at the lowest airmass during our allotted telescope time; this includes 7 low-luminosity and 7 high-luminosity sources (Table 1 and Figure 1).

3. FIELD SPECTROSCOPY

We used the SDSS g, r, i, z imaging to choose targets for our multi-object spectroscopy. Empirical color distributions at the redshift of each radio galaxy were determined using the SDSS spectroscopic database (e.g., Auger 2008). All of the galaxies in the field of the radio galaxy that did not already have a redshift from SDSS were given a priority based on Gaussian weights from the

empirical color distributions,

$$\text{weight} \propto e^{\frac{-\Delta_c^2}{2\sigma_c^2}},$$

where Δ_c is the difference between the observed color and the mean of the color distribution and σ_c is the quadrature sum of the width of the color distribution and the errors on the SDSS photometry. Higher priority was given to galaxies with r less than one magnitude brighter and 2.5 magnitudes fainter than the radio galaxy. Slitmasks were made to optimize the number of high priority objects and the remaining space on the slitmasks was filled using the lower-priority objects.

Our spectroscopy of the fields of the radio galaxies was obtained with the Low-Resolution Imaging Spectrometer (LRIS; Oke et al. 1995) on the Keck I telescope (Table 2). All of the observations employed the 300/5000 grism on the blue side with dispersion $\sim 1.41 \text{ \AA pix}^{-1}$, the 600/10000 grating with dispersion $\sim 1.25 \text{ \AA pix}^{-1}$ on the red side, and the 680 dichroic to split the beam. The conditions were typically clear with seeing $\sim 0''.7$ for all of the observations. The multi-slit data were reduced using an automated pipeline written in Python (Auger, *in prep.*). This pipeline removes the bias and overscan regions of the CCDs and flatfields the data. It then automatically determines a mask distortion and wavelength solution using the flatfield images, arclamp exposures, and night skylines. The spectra are resampled and individual exposures are coadded, then spectral traces are extracted using a flux-weighted aperture. Redshifts were determined by cross-correlating the extracted spectra with galactic and stellar template spectra, and all of these redshifts were verified by eye. If the cross-correlation failed, redshifts were determined by manually identifying features; the typical errors from the cross-correlation and manual identification are $\Delta z \sim 0.0003$. Manual identification was necessary for only $\sim 8\%$ of the objects, most of which are at $z > 0.7$. These objects tend to require manual redshifts for two reasons: the correlation templates are redshifted to wavelengths where artifacts from skylines can confuse the cross-correlation, and the templates do not extend sufficiently blueward to cover the Mg and Fe absorption features sometimes seen in these spectra. The number of successful redshifts obtained per mask is listed in Table 2. These redshifts were added to the galaxies with SDSS redshifts in each field to create redshift catalogs for the fields of the 14 radio galaxies.

4. ANALYSIS AND RESULTS

We use the iterative group finding algorithm of Auger et al. (2007) to determine group membership for each of the radio galaxy groups. The algorithm requires an initial estimate of the velocity dispersion, which we take to be a typical poor cluster dispersion of 700 km s^{-1} , and defines the group membership by requiring that all group galaxies be clustered spatially and kinematically. The iterative method determines group velocity dispersions using the gapper algorithm when the group has fewer than 15 members and the biweight statistic when the group has 15 or more members (e.g., Beers et al. 1990), and the group center is the mean position of the group galaxies. The errors on the velocity dispersions are determined from a bootstrap resampling and the offset

TABLE 1
MODERATE REDSHIFT RADIO GALAXY SUB-SAMPLE

Radio Galaxy	R. A.	Dec	Redshift	$L_{1.4\text{GHz}}$ $10^{24} \text{ W Hz}^{-1}$
125622.106+012535.08	12 56 22.11	+01 25 35.1	0.3346	22.86
141652.862+120227.14	14 16 52.86	+12 02 27.1	0.3344	3.41
144020.784+112507.09	14 40 20.78	+11 25 07.1	0.3109	20.50
155437.010+374406.03	15 54 37.01	+37 44 06.0	0.3956	22.70
165059.834+190110.02	16 50 59.83	+19 01 10.0	0.3203	3.88
170653.810+230903.52	17 06 53.81	+23 09 03.5	0.3295	3.53
213739.115−081403.44	21 37 39.12	−08 14 03.4	0.3416	1.91
222821.192+011412.29	22 28 21.19	+01 14 12.3	0.2934	2.09
223616.932−100045.54	22 36 16.93	−10 00 45.5	0.3296	2.95
232844.520+000134.32	23 28 44.52	+00 01 34.3	0.2921	3.59
234509.821−100946.50	23 45 09.82	−10 09 46.5	0.2923	12.90
011425.594+002932.59	01 14 25.59	+00 29 32.6	0.3546	17.01
013352.730+011343.63	01 33 52.73	+01 13 43.6	0.3081	14.39
021437.167+004235.36	02 14 37.17	+00 42 35.4	0.2902	15.32

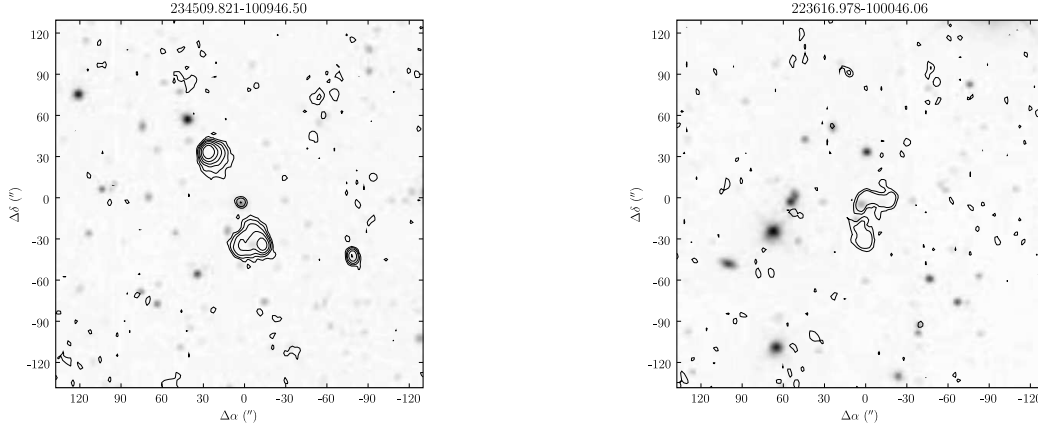


FIG. 1.— FIRST radio contours overlaid on the SDSS r optical imaging for the radio galaxies 234509.821−100946.50 (a typical high-power source, *left*) and 223616.978−100045.54 (a typical low-power source, *right*). Images for all 14 of the radio galaxies are available in the electronic edition.

TABLE 2
LRIS MOS OBSERVATIONS

Radio Galaxy	Observation Date	Exposure Time (s)	# of Redshifts
125622.106+012535.08	2007 Jun 11	3600	26
141652.862+120227.14	2007 Jun 11	3600	30
144020.784+112507.09	2007 Jun 11	3600	30
155437.010+374406.03	2007 Jun 11	3600	24
165059.834+190110.02	2007 Jun 11	3000	27
170653.810+230903.52	2007 Jun 11	3000	27
213739.115−081403.44	2007 Jul 14	2400	27
222821.192+011412.29	2007 Jul 15	2400	22
223616.978−100046.06	2007 Jun 11	2700	22
	2007 Jul 14	2400	19
232844.518+000133.64	2007 Jun 12	3600	22
	2007 Jul 15	2400	20
234509.821−100946.50	2007 Jul 14	2400	22
011425.594+002932.59	2007 Jul 14	2400	22
013352.730+011343.63	2007 Jul 15	2400	26
021437.167+004235.36	2007 Jul 15	2400	23

to the radio galaxy is with respect to the centroid of the group. The group properties of the 14 radio galaxies are listed in Table 3, and the properties of the members of each group are tabulated in Table 4.

We have investigated several correlations between the radio luminosity and the group characteristics, including: the number of spectroscopically confirmed group members (Figure 2a); the group velocity dispersion (Figure 2b); the radio galaxy transverse offset from the group center (Figure 2c); the radio galaxy kinematic offset from the group center (Figure 2d); and the distance from the radio galaxy to the closest group member (Figure 2e). All of these properties are consistent with being uncorrelated with the radio luminosity. Furthermore, a Kolmogorov-Smirnov test cannot distinguish between the low-luminosity and high-luminosity subsamples for any of these properties.

Our spectroscopic completeness varies substantially across the 14 fields as a result of only obtaining one slit-mask in each field. We therefore use the SDSS photometry to also characterize the radio galaxy environments. We use the priorities assigned to our spectroscopic targets to create a probability distribution that describes the likelihood that a galaxy with a given priority is spectroscopically found to be at the same redshift as the radio galaxy. We fit a smooth analytic form to the empirical distribution and assign probabilities to all of the galaxies in the field of each radio galaxy based upon their

TABLE 3
RADIO GALAXY GROUP PROPERTIES

Name	R. A.	Dec	N_{spec}	N_{500}	N_{1000}	Offset ($''$)	z	σ_{group} (km s^{-1})
125622.106+012535.08	12 56 21.56	+01 25 46.4	21	17	30	14	0.3351	390 ± 110
141652.862+120227.14	14 16 53.33	+12 02 14.9	12	7	18	14	0.3340	400 ± 60
144020.784+112507.09	14 40 20.62	+11 25 15.7	16	15	33	9	0.3132	710 ± 100
155437.010+374406.03	15 54 36.83	+37 45 39.6	10	9	24	94	0.3944	510 ± 200
165059.834+190110.02	16 50 59.78	+19 01 46.8	10	11	23	37	0.3234	580 ± 160
170653.810+230903.52	17 06 52.51	+23 08 29.7	12	12	30	38	0.3286	320 ± 60
213739.115+081403.44	21 37 37.78	+08 14 23.0	25	26	45	28	0.3413	640 ± 90
222821.192+011412.29	22 28 22.21	+01 13 50.0	4	5	13	27	0.2951	930 ± 320
223616.932+100045.54	22 36 17.16	+10 00 17.8	7	6	18	28	0.3303	530 ± 100
232844.520+000134.32	23 28 45.39	+00 01 01.8	8	8	21	35	0.2940	640 ± 210
234509.821+100946.50	23 45 02.71	+10 11 02.6	8	11	34	130	0.2903	650 ± 150
011425.594+002932.59	01 14 25.40	+00 29 19.9	15	14	28	13	0.3534	440 ± 200
013352.730+011343.63	01 33 53.37	+01 13 38.6	4	7	18	11	0.3075	230 ± 70
021437.167+004235.36	02 14 37.84	+00 43 10.9	9	11	23	37	0.2894	140 ± 40

NOTE. — Col. (1): Name of radio galaxy. Col. (2): Right Ascension in hours, minutes, and second. Col. (3): Declination in degrees, arcminutes, and arcseconds. Col. (4): Number of spectroscopically confirmed group members. Col. (5): Number of photometrically estimated group members within $500 \text{ h}^{-1} \text{ kpc}$. Col. (6): Number of photometrically estimated group members within $1 \text{ h}^{-1} \text{ Mpc}$. Col. (7): Offset of the radio galaxy from the spectroscopic group center. Col. (8): Redshift of the group. Col. (9): Velocity dispersion of the group.

TABLE 4
GROUP MEMBER PROPERTIES

Name	R. A.	Dec	Redshift	g	r	i	z
125622.106+012535.08	12 56 30.804	01 25 04.836	0.3327	21.906	20.665	19.951	19.700
	12 56 16.982	01 25 30.720	0.3329	22.788	20.461	19.831	19.380
	12 56 30.506	01 26 02.724	0.3332	20.955	19.477	18.942	18.665
	12 56 14.794	01 25 44.256	0.3335	22.096	20.519	19.889	19.535
	12 56 27.386	01 26 44.016	0.3338	22.446	20.671	20.053	19.558
	12 56 23.198	01 25 05.916	0.3338	21.727	20.295	19.667	19.337
	12 56 25.534	01 26 26.808	0.3339	22.385	20.604	20.056	19.711
	12 55 54.360	01 23 27.994	0.3340	20.082	18.378	17.795	17.384
	12 56 20.503	01 26 52.620	0.3341	22.822	21.195	20.606	20.234
	12 56 22.106	01 25 35.148	0.3346	19.711	17.880	17.261	16.895
	12 56 13.978	01 25 04.908	0.3346	20.498	18.804	18.198	17.882
	12 56 15.804	01 26 51.288	0.3347	21.017	19.401	18.751	18.442
	12 56 26.422	01 26 05.244	0.3349	22.913	21.571	21.087	20.769
	12 56 18.802	01 25 23.160	0.3351	22.184	20.485	19.896	19.588
	12 56 16.642	01 26 30.444	0.3354	21.866	20.268	19.621	19.356
	12 56 36.026	01 26 33.072	0.3358	21.852	20.592	20.196	19.940
	12 56 34.111	01 26 22.236	0.3360	22.360	21.300	20.704	20.520
	12 56 24.034	01 25 14.304	0.3377	22.575	21.073	20.371	19.888
	12 56 21.091	01 25 01.272	0.3378	21.853	20.517	19.913	19.496
	12 56 27.929	01 25 57.396	0.3392	20.839	19.061	18.517	18.189
	12 56 11.810	01 25 36.156	0.3402	21.761	20.067	19.455	18.947

NOTE. — Group member properties for the group associated with the radio galaxy 125622.106+012535.08. Group member properties for all 14 systems are available in the electronic edition. Col. (1): Name of radio galaxy. Col. (2): Right Ascension in hours, minutes, and seconds. Col. (3): Declination in degrees, arcminutes, and arcseconds. Col. (4): Galaxy redshift. Cols. (5-8): SDSS g, r, i, z magnitudes.

previously determined spectroscopic priority. We sum the probabilities of all galaxies within $500 \text{ h}^{-1} \text{ kpc}$ and $1 \text{ h}^{-1} \text{ Mpc}$ of the radio galaxies to determine the expected number of galaxies at the redshifts of the radio galaxies, N_{500} and N_{1000} . These values are collected in Table 3 and provide further evidence that the radio galaxy luminosity is not correlated with the density of galaxies (Figure 3).

We have also investigated the relationship between other radio properties of the radio galaxy and the environment. The core-to-lobe flux ratio and the angular extent of the radio emission were computed using the sources detected in FIRST. We note that the FIRST data may not include resolved-out extended emission and the

lobe fluxes may therefore be underestimated. However, we do not find any significant correlation between the properties of the environment and the core-to-lobe flux ratio or the angular extent of the radio galaxy.

5. DISCUSSION

Geach et al. (2007) have examined the environments of a set of four radio galaxies at redshifts $z \sim 0.35$ and $z \approx 0.65$ with spectroscopy and X-ray observations. This sample includes three galaxies that we would classify as low-power and one higher-power radio galaxy, and the sample spans a range of environments. We note, however, that none of the galaxies in our sample or the Geach et al. (2007) sample are truly isolated; all have at least two spectroscopic companions. This could be due

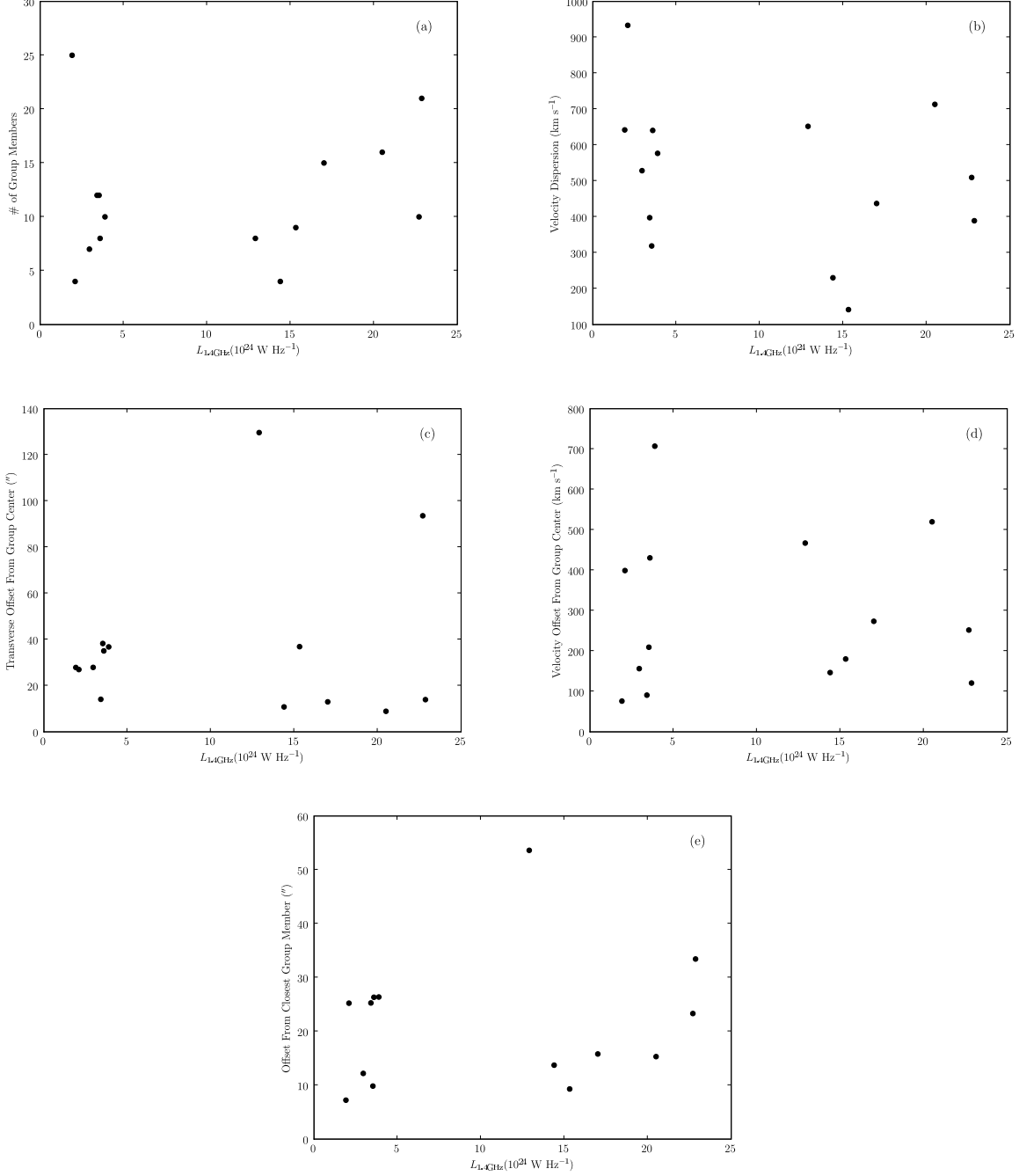


FIG. 2.— Relation between the radio galaxy luminosity and various group properties, including: (a) number of group members; (b) velocity dispersion of the group; (c) transverse offset of the radio galaxy from the group center; (d) kinematic offset of the radio galaxy from the group center; and (e) the distance from the radio galaxy to the closest group member.

to selection effects. Geach et al. (2007) investigated radio galaxies that appeared to have a red sequence, while our sample required the galaxy to be in the SDSS spectroscopic sample. The SDSS preferentially observes more luminous galaxies at higher redshifts, and these galaxies tend to exist in over-dense environments. However, photometric surveys of purely radio-selected galaxies have also suggested that nearly all radio-galaxies reside in groups (e.g., Allington-Smith et al. 1993), and we therefore do not expect this bias to be significant.

Our results spectroscopically support the results from photometric surveys of radio galaxies; low-luminosity and high-luminosity sources tend to exist in the same environments at moderate redshifts. The dichotomy in environments at low redshifts is likely due to the density of the intergalactic medium (IGM); high luminosity galaxies tend to have large extended lobes that do not form if the IGM is too dense (e.g., Prestage & Peacock 1988). The absence of this dichotomy at higher redshift is probably results from cosmological evolution of the

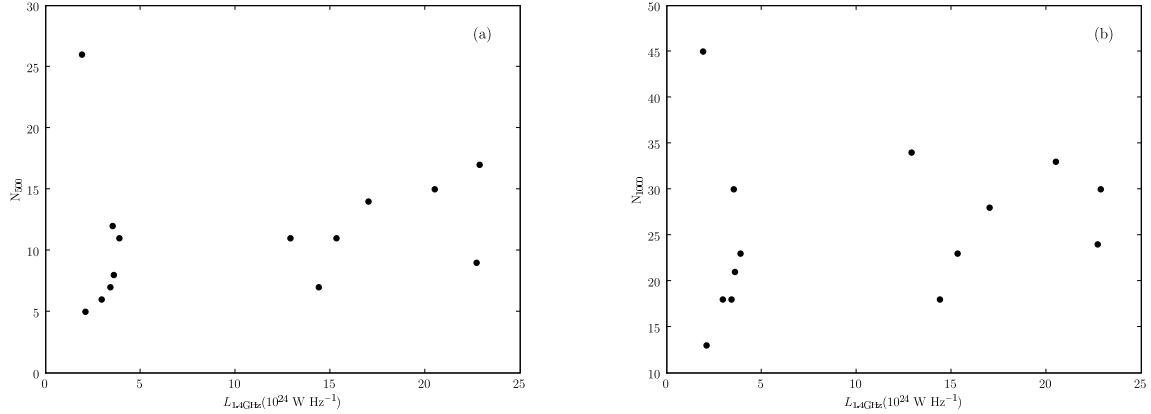


FIG. 3.— Relation between the radio galaxy luminosity and a photometric estimate of the number of group members associated with the radio galaxy within (a) $500 \text{ h}^{-1} \text{ kpc}$ and (b) $1 \text{ h}^{-1} \text{ Mpc}$.

density of the IGM (e.g., Ettori et al. 2004).

There is a substantial amount of scatter in the properties of the radio galaxy environments, though the typical radio galaxy is in a group with approximately 12 members and a velocity dispersion of $\sim 500 \text{ km s}^{-1}$. The systems 222821.192+011412.29 and 013352.730+011343.63 are found to have only 3 companions in addition to the radio galaxy. These systems may not belong to bound groups but rather may be embedded in filaments; the large velocity spread for the low-luminosity system 222821.192+011412.29 further supports this conclusion. We therefore conclude that at moderate redshifts, radio galaxies reside in all types of environments, from filaments to clusters, without regard to the radio luminosity. Belsole et al. (2007) reach a similar conclusion from a study of the X-ray environments of higher redshift radio galaxies and quasars. Thus, while radio galaxies are shown to trace large-scale-structure, they are not useful for targeting environments with specific properties (e.g., lower velocity dispersion or less rich environments) at higher redshifts.

We would like to thank Lori Lubin for helpful com-

ments. Many of the data presented herein were obtained at the W.M. Keck Observatory, which is operated as a scientific partnership among the California Institute of Technology, the University of California and the National Aeronautics and Space Administration. The Observatory was made possible by the generous financial support of the W.M. Keck Foundation. The authors wish to recognize and acknowledge the very significant cultural role and reverence that the summit of Mauna Kea has always had within the indigenous Hawaiian community. We are most fortunate to have the opportunity to conduct observations from this mountain. This work has made extensive use of the SDSS database. Funding for the SDSS and SDSS-II has been provided by the Alfred P. Sloan Foundation, the Participating Institutions, the National Science Foundation, the U.S. Department of Energy, the National Aeronautics and Space Administration, the Japanese Monbukagakusho, the Max Planck Society, and the Higher Education Funding Council for England.

REFERENCES

- Aarseth, S. J., & Fall, S. M. 1980, *ApJ*, 236, 43
 Aceves, H., & Velázquez, H. 2002, *Revista Mexicana de Astronomía y Astrofísica*, 38, 199
 Adelman-McCarthy, J. K., et al. 2007, *ApJS*, 172, 634
 Allington-Smith, J. R., Ellis, R., Zirbel, E. L., & Oemler, A. J. 1993, *ApJ*, 404, 521
 Auger, M. W., Fassnacht, C. D., Abrahamse, A. L., Lubin, L. M., & Squires, G. K. 2007, *AJ*, 134, 668
 Auger, M. W., Fassnacht, C. D., Wong, K. C., Thompson, D., Matthews, K., & Soifer, B. T. 2008, *ApJ*, in press (arXiv:0710.1650)
 Auger, M. W. 2008, *MNRAS*, 383, L40
 Bahcall, J. N., Kirhakos, S., Saxe, D. H., & Schneider, D. P. 1997, *ApJ*, 479, 642
 Bahcall, N. A., & Chokshi, A. 1992, *ApJ*, 385, L33
 Barnes, J. 1985, *MNRAS*, 215, 517
 Becker, R. H., White, R. L., & Helfand, D. J. 1995, *ApJ*, 450, 559
 Beers, T. C., Flynn, K., & Gebhardt, K. 1990, *AJ*, 100, 32
 Belsole, E., Worrall, D. M., Hardcastle, M. J., & Croston, J. H. 2007, *MNRAS*, 385
 Best, P. N. 2004, *MNRAS*, 351, 70
 Blanton, E. L., Gregg, M. D., Helfand, D. J., Becker, R. H., & Leighly, K. M. 2001, *AJ*, 121, 2915
 Blanton, E. L., Gregg, M. D., Helfand, D. J., Becker, R. H., & White, R. L. 2003, *AJ*, 125, 1635
 Bower, R. G., & Balogh, M. L. 2004, *Clusters of Galaxies: Probes of Cosmological Structure and Galaxy Evolution*, 326
 Carlberg, R. G., Yee, H. K. C., Morris, S. L., Lin, H., Hall, P. B., Patton, D. R., Sawicki, M., & Shepherd, C. W. 2001, *ApJ*, 563, 736
 Colless, M., et al. 2001, *MNRAS*, 328, 1039
 Collister, A. A., & Lahav, O. 2005, *MNRAS*, 361, 415
 Condon, J. J., Cotton, W. D., Greisen, E. W., Yin, Q. F., Perley, R. A., Taylor, G. B., & Broderick, J. J. 1998, *AJ*, 115, 1693
 Conselice, C. J., Bershad, M. A., Dickinson, M., & Papovich, C. 2003, *AJ*, 126, 1183
 Deltorn, J.-M., Le Fevre, O., Crampton, D., & Dickinson, M. 1997, *ApJ*, 483, L21
 Ettori, S., Tozzi, P., Borgani, S., & Rosati, P. 2004, *A&A*, 417, 13
 Fanaroff, B. L., & Riley, J. M. 1974, *MNRAS*, 167, 31P
 Fassnacht, C. D., et al. 2007, submitted to *ApJ*

- Geach, J. E., Simpson, C., Rawlings, S., Read, A. M., & Watson, M. 2007, *MNRAS*, 373
- Gerke, B. F., et al. 2005, *ApJ*, 625, 6
- Heckman, T. M., Smith, E. P., Baum, S. A., van Breugel, W. J. M., Miley, G. K., Illingworth, G. D., Bothun, G. D., & Balick, B. 1986, *ApJ*, 311, 52
- Hill, G. J., & Lilly, S. J. 1991, *ApJ*, 367, 1
- Huchra, J. P., & Geller, M. J. 1982, *ApJ*, 257, 423
- Iono, D., Yun, M. S., & Mihos, J. C. 2004, *ApJ*, 616, 199
- Lilly, S. J., & Prestage, R. M. 1987, *MNRAS*, 225, 531
- Lin, L., et al. 2004, *ApJ*, 617, L9
- Mihos, J. C., Richstone, D. O., & Bothun, G. D. 1992, *ApJ*, 400, 153
- Miley, G. K., et al. 2006, *ApJ*, 650, L29
- Miller, N. A., Owen, F. N., Burns, J. O., Ledlow, M. J., & Voges, W. 1999, *AJ*, 118, 1988
- Miller, N. A., Ledlow, M. J., Owen, F. N., & Hill, J. M. 2002, *AJ*, 123, 3018
- Momcheva, I., Williams, K., Keeton, C., & Zabludoff, A. 2006, *ApJ*, 641, 169
- Mulchaey, J. S., Lubin, L. M., Fassnacht, C., Rosati, P., & Jeltema, T. E. 2006, *ApJ*, 646, 133
- Oke, J. B., et al. 1995, *PASP*, 107, 375
- Padilla, N. D., et al. 2004, *MNRAS*, 352, 211
- Patton, D. R., et al. 2002, *ApJ*, 565, 208
- Prestage, R. M., & Peacock, J. A. 1988, *MNRAS*, 230, 131
- Ramella, M., Geller, M. J., & Huchra, J. P. 1989, *ApJ*, 344, 57
- Tully, R. B. 1987, *ApJ*, 321, 280
- Venemans, B. P., et al. 2007, *A&A*, 461, 823
- Weinmann, S. M., van den Bosch, F. C., Yang, X., & Mo, H. J. 2006, *MNRAS*, 366, 2
- Williams, K. A., Momcheva, I., Keeton, C. R., Zabludoff, A. I., & Lehar, J. 2006, *ApJ*, 646, 85
- Wilman, D. J., Balogh, M. L., Bower, R. G., Mulchaey, J. S., Oemler, A., Carlberg, R. G., Morris, S. L., & Whitaker, R. J. 2005a, *MNRAS*, 358, 71
- York, D. G., et al. 2000, *AJ*, 120, 1579
- Zabludoff, A. I., & Mulchaey, J. S. 1998, *ApJ*, 496, 39
- Zirbel, E. L. 1997, *ApJ*, 476, 489